EPJ manuscript No.
(will be inserted by the editor)

Quantum chaos of dark matter in the Solar System

D.L. Shepelyansky[1]

Laboratoire de Physique Théorique du CNRS, IRSAMC, Université de Toulouse, CNRS, UPS, 31062 Toulouse, France

Dated: 17 Dec 2017; updated: January 22, 2017

Abstract. We perform time-dependent analysis of quantum dynamics of dark matter particles in the Solar System. It is shown that this problem has similarities with a microwave ionization of Rydberg atoms studied previously experimentally and analytically. On this basis it is shown that the quantum effects for chaotic dark matter dynamics become significant for dark matter mass ratio to electron mass being smaller than 2×10^{-15}. Below this border multiphoton diffusion over Rydberg states of dark matter atom becomes exponentially localized in analogy with the Anderson localization in disordered solids. The life time of dark matter in the Solar System is determined in dependence on mass ratio in the localized phase and a few photon ionization regime. The quantum effects for dark matter captured by other binary systems are also discussed.

PACS. XX.XX.XX No PACS code given

1 Introduction

The properties of dark matter are now actively discussed by the astronomy community (see e.g. [1]). Recently, a necessity of correct description of galactic structures, in particularly singular density cusp problem, attracted a growing interest to the ultralight dark matter particles (DMP) of bosons with a mass $m_d \sim 10^{-22} eV$ (see e.g. [2,3,4,5] and Refs. therein). However, the mass m_d of light DMP is unknown and possibilities of its detection are under active discussions [2,6]. At small values of m_d (or its ratios to electron mass m_e) the quantum effects start to be dominant [4,5,7]. Till present the quantum effects have been studied in the frame of static solutions of Schrödiner and Poisson equations.

In this work we perform a time-dependent analysis of quantum effects for light DMP which dynamics takes place in binary rotating systems. The properties of quantum dynamics of such DMP in the Solar System (SS), its atomic Rydberg structure (similar to hydrogen atom) and multiphoton ionization (escape from SS) are analyzed here for SS and more generic binary systems. For the SS we consider the model of Sun with Jupiter which creates a time periodic perturbation leading to dynamical chaos and diffusion of DMP energy with eventual escape (or ionization) from the SS. In the quantum case the periodic gravitational force, created by rotation of Jupiter, leads to absorption or emission of photons changing the DMP energy by integers of $\hbar\omega_J$ where the frequency $\omega_J = 2\pi/T_J$ is determined by the period of Jupiter rotation. We call these energy quanta as photons even if there are no electromagnetic forces in this system (a reader can also look on these quanta as gravitons).

Below we show that for a light DMP mass with $m_d/m_e < 2 \times 10^{-15}$ the quantum effects start to play a dominant role and that they lead to a dynamical localization of diffusive chaotic motion of DMP in binary system being similar to the Anderson localization in disordered solids (see [8,9,10]). Due to localization a DMP escape from SS is strongly suppressed and DMP life time in SS is increased enormously. A similar dynamical localization of chaotic diffusion of multiphoton transitions has been predicted for microwave ionization of excited hydrogen and Rydberg atoms and observed in experiments (see [11,12,13, 14,15] and Refs. therein). We show that the DMP ionization from SS induced by Jupiter has many similarities with physics of multiphoton ionization of atoms in strong laser fields [16] and properties of Rydberg atoms in external fields [17]. Since the classical DMP dynamics in SS is mainly chaotic the quantum evolution of DMP has many properties of quantum chaos [18]. We show that one of the consequences of classical and quantum chaos in binary systems is an absence of singular density cusp in center of a binary.

2 Kepler map description of classical DMP dynamics

We consider the restricted three-body problem [19] with a DMP of light mass m_d, Sun of mass M and a planet (Jupiter) of mass m_p moving around Sun over a circular orbit of radius r_p with velocity v_p and frequency $\omega_p = v_p/r_p$. For the Jupiter case we have $v_J = v_p = 13.1 km/s$, $r_J = r_p = 7.78 \times 10^8 km = 5.204 ASTRU$ (ASTRU is for astronomy units), orbital period $T_p = 2\pi/\omega_p = 11.8 yrs$

and $m_p/M = 1/1047$ [20]. The studies of DMP dynamics in a binary system with $m_p \ll M$ showed that the dynamics of comets or DMP is well described by the generalized Kepler map [21,22,23,24,25,26,27,28]:

$$E_{n+1} = E_n + F(\phi_n) \; , \qquad (1)$$
$$\phi_{n+1} = \phi_n + 2\pi |2E_{n+1}/(m_d {v_p}^2)|^{-3/2} \; ,$$

where E_n is DMP energy, ϕ_n is Jupiter phase taken at n-th passage of DNP through perihelion on a distance q from Sun. This symplectic map description is well justified for $q > r_p$ where the kick function $F(\phi) = f_0(m_p/M)m_d {v_p}^2 \sin\phi$ and $f_0 \approx 2(r_p/q)^{1/4}\exp(-0.94(q/r_p)^{3/2})$. For $q \sim r_p$, like for the comet Halley case, the function $F(\phi)$ contains also higher harmonics with a maximal kick amplitude $f_0 \approx 2.5$ for the comet Halley [22,27]. The map is valid when the orbital DMP period is larger than the planet period. This map generates a chaotic DMP dynamics similar to those of the Chirikov standard map [29,30] for energy being below the chaos border $|E| < E_{ch} = w_{ch} m_d {v_p}^2/2$ with $w_{ch} \approx 2.5(2f_0 m_p/M)^{2/5}$. Examples of Poincaré sections for the generalized Kepler map are given in [22,27,28]. For the case of Jupiter with $\sin-$kick function we have $w_{ch} \approx 0.3$ while for the comet Halley case with a few harmonics one finds $w_{ch} \approx 0.45$. In the chaotic phase the energy is growing in a diffusive way with number of DMP orbital periods t_{orb}: $(\Delta E)^2 \approx D t_{orb}$. The diffusion coefficient D is approximately given by the random phase approximation for phase ϕ:

$$D \approx < F^2(\phi) > \approx {f_0}^2 (m_p/M)^2 {m_d}^2 {v_p}^4/2 \; . \qquad (2)$$

For a DMP orbit with initial energy about $-m_d {v_p}^2/2$ the ionization energy is $E_I = m_d v_p^2/2$ and a diffusive ionization time (escape from SS) is approximately $t_D \approx 2\pi r_p {E_I}^2/(v_p D)$ that gives for SS with Jupiter $t_D \approx 3 \times 10^6 yrs$. More detailed numerical simulations with many DMP trajectories, including the case of comet Halley, give a typical time scale $t_I \approx t_H \approx 10^7 yrs \sim t_D$ [22,26]. For an external galactic DMP flow scattering on SS, DPM are captured and accumulated during the time scale t_H. After this time scale the DMP distribution in SS reaches a steady-state when the capture process is compensated by escape on a time scale t_I. The capture process and its cross-section are discussed in detail in [31,32,26].

It is also useful to note that a rotating planet corresponds to a rotating dipole in the Coulomb problem which can be transformed to a circular polarized monochromatic field appearing in the problem of microwave ionization of Rydberg atoms and autoionization of molecular Rydberg states [33].

3 "Hydrogen" atom of dark matter

Since the gravitational interaction is similar to the Coulomb interaction we directly obtain from [34] the levels of dark matter atom with the Bohr radius $a_{Bd} = \hbar^2/(\kappa {m_d}^2 M) = 1.01 \times 10^{-26} cm (m_e/m_d)^2$ for SS and energy levels $E_{dn} = -E_{Bd}/(2n^2)$ where κ is the gravitational constant. Here we have the dark matter atomic energy $E_{Bd} = \kappa m_d M/a_{Bd} = 7.47\times 10^{36}(m_d/m_e)^3 ev$ and related atomic frequency $\omega_{Bd} = E_{Bd}/\hbar = \kappa^2 {m_d}^3 M^2/\hbar^3$. For the SS we have the Bohr radius $a_{Bd} = 1.30 \times 10^{-40}(m_e/m_d)^2 r_J$ so that $a_{Bd} = r_J$ at $m_d/m_e = 1.14 \times 10^{-20}$. Thus we have $E_{Bd} = 1.10 \times 10^{-23} ev = \hbar\omega_J$ when $a_{Bd} = r_J$ and one photon energy of Jupiter frequency $\omega_J = \omega_p = v_p/r_p$ is $\hbar\omega_J$. Hence one needs $N_J = E_{Bd}/(2\hbar\omega_J) = 3.38 \times 10^{59}(m_d/m_e)^3 = 0.5$ photons to ionize the ground state of DMP atom at this mass ratio.

4 Quantum Kepler map and Anderson localization

In analogy with the microwave ionization of excited hydrogen and Rydberg atoms [12,15] the quantum dynamics of DPM is described by the quantum Kepler map obtained from (2) by replacing the classical variables (E, ϕ) by operators $\hat{E} = \hbar\omega_p \hat{N}$, $\hat{\phi}$ with a commutator $[\hat{N}, \hat{\phi}] = -i$. Here N has the meaning of a number of photons absorbed or emitted due to interaction with periodic perturbation of planet. The quantum Kepler map has the form [12,15]:

$$\bar{\hat{N}} = \hat{N} + k \sin\hat{\phi} \; , \bar{\hat{\phi}} = \hat{\phi} + 2\pi\omega(-2\omega\bar{\hat{N}})^{-3/2} \; , \qquad (3)$$

where bars mark new values of operator variables after one orbital period of DMP and a kick amplitude $k = f_0 m_p m_d {v_p}^2/(\hbar\omega_p M) = 2f_0(m_p/M)N_I = 2.10\times 10^{17}(m_d/m_e)$ gives the maximal number of absorbed/emitted photons after one kick (numbers are given for Jupiter case). Here we express the planet frequency ω_p in atomic units of dark matter atom with $\omega = \omega_p/\omega_{Bd} = 1.48 \times 10^{-60}(m_e/m_d)^3$. The corresponding wavefunction evolution in the basis of photons N is described by the map which is similar to the quantum Chirikov standard map [12,15]:

$$\bar{\psi}_{N_\phi} = \exp(-k\cos\phi)\exp(-iH_0(N_\phi))\psi_{N_\phi} \qquad (4)$$

with $H_0(N_\phi) = 2\pi(-2\omega(N_0+N_\phi))^{-1/2}$ and $N = N_0 + N_\phi$, where N_0 is the number of photons of DMP initial state. For the initial DMP state with energy $E_d = -m_d v_p^2/2$ we have the number of photons required for DMP ionization being

$$N_I = m_d v_p^2/(2\hbar\omega_p) = 4.39 \times 10^{19} m_d/m_e \qquad (5)$$

with $N_0 = -N_I$ and the right equality given for the Jupiter case at $f_0 = 2.5$. In this expression for N_I we use $w_{ch} \approx 1$ and assume that $a_{Bd} < r_J$. For $a_{Bd} > r_J$ the minimal energy of DMP is given by the ground state $E = -E_{Bd}/2$.

The quantum interference effects lead to exponential localization of chaotic diffusion being similar to the Anderson localization in disordered solids [9,10]. In analogy with the microwave ionization of hydrogen atoms, the localization length expressed in the number of photons is

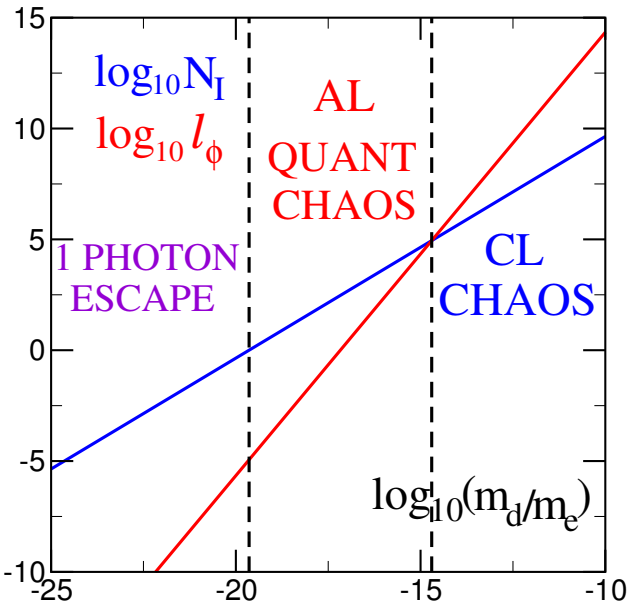

Fig. 1. Dependence of number of photons N_I of Jupiter frequency required for ionization (escape) of DMP on its mass m_d rescaled by electron mass m_e (blue line given by the analytic expression (5)), dependence of Anderson localization length of quantum chaos ℓ_ϕ on m_d/m_e (red line given by the analytic expression (6)); vertical dashed lines mark regimes of different ionization mechanisms of DMP: one photon escape (left), Anderson localization (middle), classical chaos with diffusive ionization (right); here initial DMP energy is $E_d = -m_d {v_J}^2/2$.

[12,15]:

$$\ell_\phi \approx D/(\hbar\omega_p)^2 \approx k^2/2 = 2{f_0}^2(m_p/M)^2{N_I}^2 \approx {f_0}^2{m_p}^2{m_d}^2{v_p}^4/2(\hbar\omega_p M)^2 \approx 2.20\times 10^{34}(m_d/m_e)^2 \quad (6)$$

where the last equality is given for the Jupiter case at $f_0 = 2.5$.

The wavefuction ψ_{N_ϕ} is exponentially localized giving a steady-state probability distribution over photonic states:

$$< |\psi_{N_\phi}|^2 > \; = \; W(N_\phi) \approx (1+2|N_\phi|/\ell_\phi)\, \exp\,(-2|N_\phi|/\ell_\phi)/2\ell_\phi. \quad (7)$$

The above expression for ℓ_ϕ is valid for $\ell_\phi > 1$ while for $\ell_\phi < 1$ we enter in the regime of perturbative localization. The steady-state localized distribution (7) is settled on a quantum time scale $t_q \approx T_p\ell_\phi$ [11,12,15].

The localization takes place for the photonic range $|N_\phi| < N_I$ and it is well visible for $\ell_\phi < N_I$. For $\ell_\phi > N_I$ a delocalization takes place and DMP escape is well described by the classical chaotic dynamics and diffusion. For Jupiter case and DMP at initial energy $E_d = -m_d v_p^2/2$, with the corresponding N_I (we assume here the chaos border $w_{ch} \approx 1$, for $w_{ch} < 1$ we should multiply N_I by w_{ch}). Thus we find that the delocalization takes place at

$$m_d/m_e > \hbar\omega_p(M/m_p)^2/({f_0}^2 m_e {v_p}^2) = 2\times 10^{-15}\,, \quad (8)$$

with the last equality given for the Jupiter case. For smaller ratios $m_d/m_e < 2.0\times 10^{-15}$ we have Anderson like localization of DMP probability on the photonic lattice. At the delocalization border with $\ell_\phi = N_I$ we have $N_I = 8.78\times 10^4$ at the above value of m_d/m_e so that the DMP ionization goes via highly multiphoton process.

An example of probability distribution for a localized state at $\ell_\phi = 1.39$ and $m_d/m_e = 7.95\times 10^{-18}$ corresponds to Fig.3 in [15]. The number of photons N_I required for ionization of an initial DMP state with energy E_d also depends on the mass ratio m_d/m_e so that one photon ionization takes place for $N_I < 1$ corresponding to $m_d/m_e < 2.28\times 10^{-20}$.

The different regimes of quantum DMP dynamics are shown in Fig. 1. The classical description is valid for $\ell_\phi > N_I$ corresponding to $m_d/m_e > 2\times 10^{-15}$, the Anderson photonic localization takes place in the range $2.28\times 10^{-20} < m_d/m_e < 2\times 10^{-15}$ and one photon ionization appears for $m_d/m_e < 2.28\times 10^{-20}$.

Even if the quantum Kepler map gives an approximate description of quantum excitation, it was shown that it provides a good description [35] of microwave ionization of real three-dimensional excited hydrogen atoms in delocalized and localized regimes [14,13]. This result justifies the given description of quantum DMP dynamics in SS.

5 Ionization times

The typical time scales of ionization (escape) for these three regimes can be estimated as follows. In the delocalized phase $\ell_\phi > N_I$ the ionization time is determined by a diffusive process with $t_I \approx t_H \approx 10^7 yrs$ as obtained from extensive numerical simulations of comet Halley [22] and classical chaotic dynamics of DMP [26]. This regime t_I is independent of m_d.

In the localized phase $\ell_\phi < N_I$ the ionization takes place only from the exponentially small tail of the steady-state probability distribution (7) with the escape rate $\Gamma \sim W \sim (N_I/\ell_\phi)\exp(-2|N_I|/\ell_\psi)$ so that we obtain the estimate for ionization time $t_I \sim 1/\Gamma$:

$$t_I \approx t_H \exp(2|N_I|/\ell_\phi - 2)/(2|N_I|/\ell_\phi - 1)\,. \quad (9)$$

The above expression assumes that $\ell_\phi > 1$ and $N_I \geq \ell_\phi$ giving $t_I = t_H$ at delocalization border $N_I = \ell_\phi$.

In the case when $N_I < 1$ an absorption of one photon with energy $\hbar\omega_p$ is sufficient to give to DMP positive energy leading to its escape on infinity or ionization. In this regime the one-photon ionization rate is $\Gamma \approx (\omega_p/2\pi)(J_1(k))^2$ where $J_1(k)$ is Bessel function. This simple estimate, following from the quantum Kepler map (4), is in a good agreement with the exact computation of one-photon ionization rate as it is demonstrated in [11,12]. Hence, the one-photon ionization time is

$$t_I \approx 1/\Gamma \approx T_p(2/k)^2 \approx 1.07\times 10^{-33}(m_e/m_d)^2 yrs\,. \quad (10)$$

Thus at one-photon border $N_I = 1$ and $m_d/m_e = 2.28\times 10^{-20}$ we have $t_I = 2.05\times 10^6 yrs$. For $2.28\times 10^{-20} <$

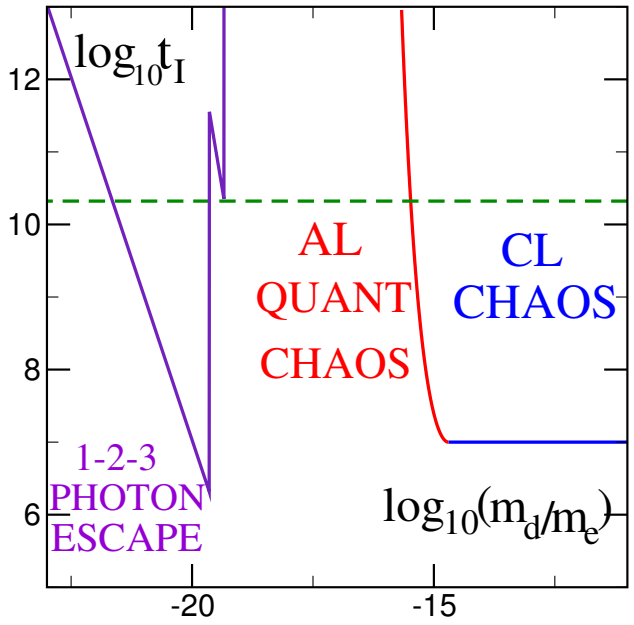

Fig. 2. Dependence of DMP escape (ionization) time t_I from the SS (expressed in years) as a function of mass ration m_d/m_e for initial DMP energy $E_d = -{m_d v_J}^2/2$. The blue horizontal line shows regime of classical escape due to chaos ($t_I \approx 10^7$ years independent of m_d/m_e), red curve shows t_I of the analytic expression (9) in the regime of Anderson localization of quantum photonic transitions, violet line shows the analytic expression (10) for t_I in the regime of 1,2 and 3 photon escape; horizontal dashed line marks the life time of Universe t_U.

$m_d/m_e < 4.56 \times 10^{-20}$ two photons are required for DMP ionization with $\Gamma = (\omega_p/2\pi)(J_2(k))^2$ and slightly above one photon ionization border we obtain $t_I \approx T_p(2/k)^4 \approx 3.6 \times 10^{12} yrs$ being much larger than the age of universe $t_U \approx 1.38 \times 10^{10} yrs$ (at the 3-photon border we have $t_I \approx 4(2/k)^6 T_p \approx 4 \times 10^{15} yrs$).

The global dependence of escape time t_I on DMP mass m_d is shown in Fig. 2. The life time is larger than the life time of Universe for the mass ratio $2.2 \times 10^{-20} < m_d/m_e < 3.4 \times 10^{16}$ where the left inequality is at the transition from 2-photon to 1-photon ionization. For $m_d/m_e < 2.8 \times 10^{-22}$ the one-photon ionization becomes very slow and we also have $t_I > t_U$. In this range we have the atomic size of DMP atom $a_{Bd} \gg r_J$ and the above ionization time is given for ionization from the ground state. The time t_I for one-photon process becomes so large because in the quantum Kepler map (4) the kick amplitude $k \propto m_d$ becomes very small.

It would be interesting to verify the above estimates for ionization rates Γ and life times t_I by the numerical simulation methods developed for computation of these quantities in microwave ionization of Rydberg atoms [36].

6 DMP capture

For the classical DMP of Galactic wind flying through SS the capture cross-section is $\sigma \approx 8\pi {r_p}^2 (v_p/v)^2$ being diverging at low positive DMP energies $E = m_d v^2/2 > 0$ in a continuum [31,26]. The captured DMP diffuse in the chaotic region up to the chaos border $w_{ch} = 2|E|/(m_d {v_p}^2)$ as discussed above (see also [26]). Due to Anderson photonic localization (6) the diffusion is localized and, comparing to the classical border w_{ch}, DMP can reach only significantly smaller quantum border values:

$$w_q \approx 2\hbar\omega_p \ell_\phi/(m_d {v_p}^2) \approx 5. \times 10^{14} (m_d/m_e) \; . \qquad (11)$$

This dependence is valid in the range $2.28 \times 10^{-20} < m_d/m_e < 2 \times 10^{-15}$. For m_d/m_e becoming smaller than the left inequality we have $\ell_\phi < 1$ and only one photon energy is absorbed with $w_q = 1.14 \times 10^{-5}$; above the right border we obtain the classical chaos border with $w_q \approx w_{ch} \sim 1$ independent of DMP mass.

According to analysis given in [26] the classical capture process of DMP continues during time $t_H \sim t_D$ after which DMP start to escape from SS. Assuming that the Galactic DMP velocity distribution has a usual Maxwell form $f(v)dv = \sqrt{54/\pi} v^2/u^3 \exp(-3v^2/u^2)dv$ with $u \approx 220 km/s$ we can estimate the captured DMP mass as [26] : $M_{cap} \sim 100 (v_p/u)^3 (m_p/M) \rho_g {r_p}^2 v_p t_H$, where $\rho_g \approx 4 \times 10^{-25} g/cm^3$ is the Galactic mass density of dark matter. In the quantum case with photonic localization we should use $t_q < t_H$ since the accumulation continues only during time on which a steady-state distribution is reached while after it the escape of DMP from SS starts to compensate ingoing DMP flow. Thus M_{cap} is significantly reduced by the factor t_q/t_H.

In the above estimate we have $M_{cap} \propto E_H \propto m_d {v_p}^2 w_H/2$ where $w_H \sim 2 f_0 (m_p/M)$ and E_H has a meaning of DMP energy which can be captured by a kick from Jupiter. In the one-photon regime with $k < 1$ at $m_d/m_e < 4.76 \times 10^{-18}$ only DMP energies with $E = m_d v^2/2 < \hbar\omega_J$ can be captured that provides an additional reduction of M_{cap}.

Finally, the Kepler map approach allows to perform extensive simulations of DMP capture process for SS and other binaries up to time scales of SS life time [26,28] with a steady-state DMP distribution reached at such times. The obtained DMP steady-state distribution has maximal volume density on a distance comparable with a size of binary without cusp singularity at $r \ll r_p$. The physical reason is rather clear: DMP diffuse only up to the chaos border $w_{ch} \sim 1$ corresponding to hallo distances from the binary center $r_h \sim r_p/w_{ch} \sim r_p$. In the regime of quantum localization we should replace w_{ch} by $w_q < w_{ch}$ so that $r_h \sim r_p/w_q \gg r_p$ becomes even larger. Thus in presence of time-dependent effects in binaries there is no cusp singularity at the binary center, both in classical and quantum cases.

7 Other binary example

Above we considered the binary case of Sun and Jupiter. However, the obtained results can be directly extended to binary systems with other parameters. As an example we consider Sagittarius A^* which is thought to be the location of a supermassive black hole (SBH) in our Galaxy

[37] with a mass $M_{bh} \approx 4 \times 10^6 M_S$. The nearby star $S2$ moving around SBH has the following characteristics [38]: the orbital period $T_{s2} \approx 15 yrs \approx 1.3 T_p$ is comparable with the period of Jupiter T_p, the semi-major axis is $r_{s2} = 980 ASTRU = 188 r_J$ and mass $m_{s2} = 15 M_S$. Hence $\omega_{s2}/\omega_J \approx 0.7$ and the velocity of $S2$ is $v_{s2}/v_J \approx 144$ or $v_{s2} \approx 1900 km/s$. Other stars around SBH are assumed to give a small perturbation, at present there masses are not know exactly [37]. With these parameters of binary composed by SBH Sagittarius A^* and the star $S2$ (assuming regime of chaotic dynamics) we obtain from (8) that the quantum effects of Anderson photonic localization start to play a role for the mass ratio $m_d/m_e < 1.7 \times 10^{-14}$, being a bit higher than for the case of Sun and Jupiter.

8 Discussion

We performed analysis of time-dependent effects for DMP quantum dynamics in binary systems. On the basis of results obtained for multiphoton ionization of Rydberg atoms we show the emergence of Anderson photonic localization for DMP with masses $m_d/m_e < 2 \times 10^{-15}$. The life times of DMP in SS are determined in the localized regime and a few photon quantum ionization regime. The obtained results determine the life time of DMP in a binary systems as a function of DMP mass and masses of binary. The probability distribution for DMP over energy is obtained for the Anderson localization regime and the capture process characteristics are determined. These features can be accessible for detectors of dark matter.

This work is supported in part by the Programme Investissements d'Avenir ANR-11-IDEX-0002-02, reference ANR-10-LABX-0037-NEXT (project THETRACOM).

References

1. G. Bertone, D. Hooper and J. Silk, *Particle dark matter: evidence, candidates and constraints*, Phys. Rep. **405**, 279 (2005).
2. J.E. Marsh, *Axion cosmology*, Phys. Rep. **643**, 1 (2016).
3. E. Calabrese and D.N. Spergel, *Ultra-light dark matter in ultra-faint dwarf galaxies*, Mon. Not. R. Astr. Soc. **460**, 4397 (2016).
4. L. Hu, J.P. Ostriker, S. Tremaine and E. Witten, *Ultralight scalars as cosmological dark matter*, Phys. Rev. D **95**, 043541 (2017).
5. J.-W. Lee, *Brief history of ultra-light scalar dar matter models*, arXiv:1704.05057[astro-ph.CO] (2017).
6. D. Blas, D.L. Nacir and S. Sibiryakov, *Ultralight dark matter resonance with binary pulsars*, Phys. Rev. Lett. **118**, 211102 (2017).
7. W. Hu, R. Barkana and A. Gruzinov, *Fuzzy cold dark matter: the wave properties of ultralight particles*, Phys. Rev. Lett. **85**, 1158 (2000).
8. P.W. Anderson, *Absence of diffusion in certain random lattices*, Phys. Rev. **109**, 1492 (1958).
9. E. Akkermans and G. Montambaux, *Mesoscopic physics of electrons and photons*, Cambridge Univ. Press, Cambridge (2007).
10. F. Evers and A.D. Mirlin, *Anderson transitions*, Rev. Mod. Phys. **80**, 1355 (2008).
11. G.Casati, B.V.Chirikov, D.L.Shepelyansky and I.Guarneri, *Relevance of classical chaos in quantum mechanics: the hydrogen atom in a monochromatic field*, Phys. Rep. **154**, 77 (1987).
12. G.Casati, I.Guarneri and D.L.Shepelyansky, *Hydrogen atom in monochromatic field: chaos and dynamical photonic localization*, IEEE Jour. Quant. Elect. **24**, 1420 (1988).
13. E.J. Galvez, B.E. Sauer, L. Moorman, P.M. Koch and D. Richards, *Microwave ionization of H atoms: breakdown of classical dynamics for high frequencies*, Phys. Rev. Lett. **61**, 2011 (1988).
14. P.M. Koch and K.A.H. van Leeuwen, *The importance of resonances in microwave "ionization" of excited hydrogen atoms*, Phys. Rep. **256**, 289 (1995).
15. D.L. Shepelyansky, *Microwave ionization of hydgoren atoms*, Scholarpedia **7(1)**, 9795 (2012).
16. N.B. Delone and V.P. Krainov, *Multiphoton processes in atoms*, Springer-Verlag, Berlin (2000).
17. T.F. Gallagher, *Rydberg atoms*, Cambridge Univ. Press, Cambridge UK (2005).
18. F. Haake, *Quantum signature of chaos*, Springer, Berlin (2010).
19. M. Valtonen and H. Karttunen, *The Three-Body Problem*, Cambridge Univ. Press, Cambridge (2005).
20. Wikipedia contributors, *Jupiter*, `https://en.wikipedia.org/wiki/Jupiter`, Wikipedia (accessed 8 Nov 2017)
21. T.Y. Petrosky, *Chaos and cometary clouds in the Solar System*, Phys. Lett. A **117**, 328 (1986).
22. B.V. Chirikov and V.V.Vecheslavov, *Chaotic dynamics of comet Halley*, Astron. Astrophys. **221**, 146 (1989).
23. M. Duncan, T. Quinn and S. Tremaine, *The long-term evolution of orbits in the solar system: a mapping approach*, Icarus **82**, 402 (1989).
24. L. Malyshkin and S. Tremaine, *Keplerian map for the planar restricted three-body problem as a model of comet evolution* , Icarus **141**, 341 (1999).
25. I.I. Shevchenko, *The Kepler map in the three-body problem*, New Astr. **16**, 94 (2011).
26. J. Lages and D.L.Shepelyansky, *Dark matter chaos in the Solar system*, Mon. Not. R. Astr. Soc. Lett. **439**, L25 (2013).
27. G. Rollin, P. Haag and J. Lages, *Symplectic map description of Halley's comet dynamics*, Phys. Lett. A **378**, 1107 (2015).
28. G. Rollin, J. Lages and D.L.Shepelyansky, *Chaotic enhancement of dark matter density in binary systems*, Astron. Astrophys. **576**, A40 (2015).
29. B.V. Chirikov, *A universal instability of many-dimensional oscillator systems*, Phys. Rep. **52**, 263 (1979).
30. A.J.Lichtenberg, M.A.Lieberman, *Regular and chaotic dynamics*, Springer, Berlin (1992).
31. I.B. Khriplovich and D.L.Shepelyansky, *Capture of dark matter by the Solar System*, Int. J. Mod. Phys. D **18**, 1903 (2009).
32. A.H.G. Peter, *Dark matter in the Solar System. I. The distribution function of WIMPs at the Earth from solar capture*, Phys. Pev. D **79**, 103531 (2009); *Dark matter in the Solar System. III. The distribution function of WIMPs at the Earth from solar capture*, Phys. Pev. D **79**, 103533 (2009).

33. F. Benvenuto, G. Casati and D.L. Shepelyansky, *Chaotic Autoionization of Molecular Rydberg States*, Phys. Rev. Lett. **72**, 1818 (1994).
34. L.D. Landau and E.M. Lifshitz, *Quantum mechanics: non-relativistic theory*, Pergamon Press, N.Y. (1974).
35. G.Casati, I.Guarneri, D.L.Shepelyansky, *Classical chaos, quantum localization and fluctuations: a unified view*, Physica A **163**, 205 (1990).
36. A. Schelle, D. Delande and A. Buchleitner, *Microwave-driven atoms: from Anderson localization to Einstein's photoeffect*, Phys. Rev. Lett. **102**, 183001 (2009).
37. Wikipedia contributors, *Sagittarius A**, `https://en.wikipedia.org/wiki/Sagittarius_A*`, Wikipedia (accessed 5 Jan 2018).
38. Wikipedia contributors, *S2 (star)*, `https://en.wikipedia.org/wiki/S2_(star)`, Wikipedia (accessed 5 Jan 2018).